Biol. Cybern. 88, 419–424 (2003)
DOI 10.1007/s00422-003-0405-y

Biological Cybernetics

Letter to the editor

Migraine aura dynamics after reverse retinotopic mapping of weak excitation waves in the primary visual cortex

M. A. Dahlem*, S. C. Müller

Otto-von-Guericke-Universität Magdeburg, Institut für Experimentelle Physik, Abteilung Biophysik, Universitätsplatz 2, 39016 Magdeburg, Germany

Received: 25 April 2002 / Accepted: 20 February 2003 / Published online: 20 May 2003

Abstract. A kinematical model for excitable wave propagation is analyzed to describe the dynamics of a typical neurological symptom of migraine. The kinematical model equation is solved analytically for a linear dependency between front curvature and velocity. The resulting wave starts from an initial excitation and moves in the medium that represents the primary visual cortex. Due to very weak excitability the wave propagates only across a confined area and eventually disappears. This cortical excitation pattern is projected onto a visual hemifield by reverse retinotopic mapping. Weak excitability explains the confined appearance of aura symptoms in time and sensory space. The affected area in the visual field matches in growth and form the one reported by migraine sufferers. The results can be extended from visual to tactile and to other sensory symptoms. If the spatiotemporal pattern from our model can be matched in future investigations with those from introspectives, it would allow one to draw conclusions on topographic mapping of sensory input in human cortex.

1 Introduction

Migraine is characterized by repeatedly occurring one-sided or pulsating headache pain, each with intense attacks with moderate to severe pain, that can inhibit daily activity or deteriorate routine physical performance. The overall lifetime prevalence of migraine is in the western population as high as 33% in women and 13% in men (Launer et al. 1999). Migraine with aura meets the criteria above plus sensory hallucinations called aura. The aura precedes the migraine headache and usually lasts for less than half an hour. Besides its clinical relevance, the aura provides an interesting phenomenon in itself because the hallucinatory impressions reveal information about human cortical organization (Richards 1971; Grusser 1995; Dahlem et al. 2000).

Patients with migraine aura experience predominantly specific visual or tactile hallucinations (Russell and Olesen 1996). The full range of possible symptoms, however, includes a multiplicity of neurological alterations, e.g., that of sensory threshold and excitability, or of muscular tone. The focus of this article is a typical visual aura, the so-called fortification. The overall form of a fortification in the visual field is sickle-shaped; it consists of a scotoma that has on the margin of its convex side a zig-zag pattern reminiscent of a baroque city rampart (Fig. 1).

Although the fortification patterns are not the most frequent disturbances, almost 50% of all illustrations of visual phenomena show a typical fortification pattern (Wilkinson and Robinson 1985). This may reflect the fact that, of all migraine auras, the fortification can be described most accurately, and it therefore is the most promising symptom to actually reveal organization in human cortex. It was shown, for example, that the human cortical magnification factor is in good agreement with the observed exponential acceleration of the fortification toward the periphery of the visual field (Grusser 1995). Furthermore, it was suggested that the zig-zag pattern reflects the topography of the orientation map in the primary visual cortex (V1). According to this view, features of the fortification, like counter-rotating zig-zag regions, reveal quantities of cortical sensor maps (e.g., pinwheel distances in V1) (Dahlem et al. 2000), if simulations can be matched with introspectives from migraine sufferers. However, besides the preexisting cortical sensor maps, additional pattern-formation principles are necessary to explain the full range of aura symptoms, as we will show here.

Correspondence to: M. A. Dahlem
(e-mail: dahlem@ifn-magdeburg.de)
**Present address*: M. A. Dahlem
Leibniz-Institut für Neurobiologie, Brenneckestr. 6, 39118 Magdeburg, Germany

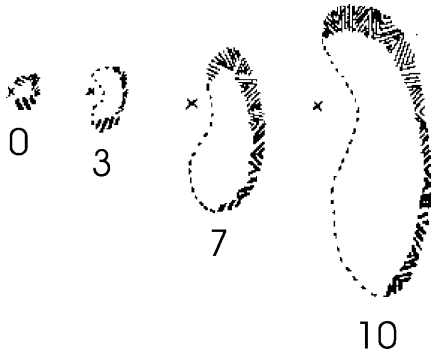

Fig. 1. Successive sketches of a scintillating scotoma, the so-called fortification. The *crosses* indicate the center of gaze, and the *numbers* state the time in minutes that passed for each fortification pattern since its first appearance close to the center of gaze. Copyright (1941) American Medical Association

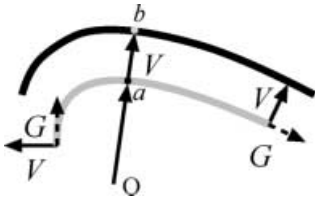

Fig. 2. A wavefront (*gray curve*) propagates according to its normal velocity V (*solid arrows*) and its tangential velocity G (*dashed arrows*). While the normal velocity is defined at any point of the *curve*, the tangential velocity describes the growth or contraction rate at the open ends. Both velocities decrease with increasing curvature of the *curve*

2 The underlying neuronal disturbance

Many aura symptoms propagate in sensory space; for example, the fortification propagates through the visual field. Lashley (1941) was the first to argue that since the symptoms propagate, a neuronal disturbance that causes them must propagate as well (Fig. 1). He calculated an average velocity of 3 mm/min for a hypothetical wave process in the primary visual cortex. Such a process can roughly account for the spatiotemporal development of typical fortification patterns in the visual hemifield. Therefore, the propagation of the visual symptoms reflects one of the fundamental organizing principles of the cortex, that is, its topographic mapping of sensory input.

Lashley's precise description of the visual symptoms of migraine aura and his speculation about their possible cause was followed by the discovery of the predicted phenomenon: epileptiform activity can induce a slowly propagating wave in the cortex (Leão 1944). The phenomenon was named cortical spreading depression (CSD) after the spread of prolonged depression of electrical activity in the cerebral cortex as measured with the electroencephalogram. It was shown later that a short phase of intense neuronal excitation precedes the depression phase (Bureš et al. 1974). This is in good agreement with the temporal order of aura symptoms: the short first phase of intense neuronal excitation causes a positive neurological symptom (zig-zag pattern), while the following depression is associated with a negative neurological symptom (scotoma). The spatiotemporal development of such waves is described in the framework of excitable media (Kapral and Showalter 1995).

3 Waves in weakly excitable media

Propagating waves of excitation can emerge in systems far from thermodynamical equilibrium. In such systems, propagation arises from local spatial coupling of nonlinear processes. The underlying nonlinearity is usually caused by autocatalysis that spreads through an extended system via diffusion of the corresponding autocatalytic species. Two striking characteristics are: the resulting excitation waves (1) have constant amplitude and (2) show no interference.

The dynamics of excitation waves in the medium can be modeled – if all reactions of the involved species are known – by a reaction-diffusion equation. In 2D media (e.g., in a shallow reaction layer), the shape of these waves can be circular or of spiral shape. Spirals evolve after a wave front is broken, which normally results in a curling of the newly created open ends. If the reactions of the reaction-diffusion system are not completely known, considerable profit comes from studying a kinematical model. Originally proposed by Wiener and Rosenbluth (1946), such a model describes the propagation of the wave front by considering the motion of curves with free ends. The attractive feature of a kinematical model is that even on a considerably smaller computational expense it perfectly mimics reaction-diffusion equations in a certain condition. This condition is called weakly excitable (Mikhailov et al. 1994).

The excitability of a medium is classified by the different shapes of the wavefront and by the front propagation. The existence of spiral-shaped waves for certain conditions in the medium defines a boundary ∂R in parameter space of excitability (Winfree 1991; Nagy-Ungvarai et al. 1994). In other words, one can observe spiral-shaped waves on one side of ∂R but not, or only temporally, on the other. In the vicinity of ∂R, the excitability is said to be weak. The spiral tip rotates in weak medium rigidly on a circular path. If excitability is increased, the rotation changes to a meandering pattern. Going toward weaker excitability in parameter space (i.e., below ∂R), the excitability eventually reaches too low a value to allow further wave propagation in the media. The boundary at which wave propagation fails is called ∂P.

Wave propagation in weakly excitable media can be modeled assuming that the normal velocity V depends at any point of the wavefront solely on the front curvature ($V = V_{(k)}$) (Zykov 1980). For wavefronts with free open ends one must consider an additional tangential velocity G (Brazhnik et al. 1988) (see Fig. 2). G can be interpreted as the growth rate of an open end. Let us now consider a curve representing the wave front at a certain time (t) and derive the fundamental kinematical equation (Mikhailov et al. 1994).

Suppose that the curvature at a point a is equal to k_a (Fig. 2). When the curve has moved in a short time interval $\mathrm{d}t$, a neighborhood of point a is transferred into the neighborhood of another point b. To calculate curvature, we introduce a local polar coordinate system (r, α) with the origin in the center of the circle of curvature from point a. In a neighborhood of point a, let the curve be given by a function $r = r(\alpha, t)$, of which the first and second derivative (r', r'') with respect to the angle α must vanish at a. In the same coordinate system, the form of the curve near point b at a time $t + \mathrm{d}t$ is given by

$$r(\alpha, t + \mathrm{d}t) = r(\alpha, t) + V(\alpha)\mathrm{d}t \tag{1}$$

When the form of a curve is known in polar coordinates, its local curvature can be determined by

$$k = (r^2 - r'^2 - rr'')(r^2 + r')^{-3/2} \tag{2}$$

Substituting Eq. 1 into Eq. 2 we obtain, to within terms of order $\mathrm{d}t$,

$$k_b = k_a - \left(k_a^2 V + k_a^2 \frac{\partial^2 V}{\partial \alpha^2}\right)\mathrm{d}t \tag{3}$$

Transforming this to differentiation with respect to the arc length s leads to

$$\mathrm{d}k \equiv k_b - k_a = -\left(k_a^2 V + \frac{\partial^2 V}{\partial s^2}\right)\mathrm{d}t \tag{4}$$

Points a and b were chosen such that they correspond to the same local polar angle α, but they have different values for their intrinsic coordinate, that is, the arc length s. That is because a circular wave propagating outwards *increases* its arc length, and, furthermore, since the arc length s is measured from the end point of a curve, the growth of the curve results in an additional shift. Due to these two effects, the arc length s of point b at a time $t + \mathrm{d}t$ has an increment

$$\mathrm{d}s = \left(\int_0^s kV\,\mathrm{d}\xi\right)\mathrm{d}t + G\mathrm{d}t \tag{5}$$

Therefore, we get

$$\mathrm{d}k = \left(\frac{\partial k}{\partial s}\right)\mathrm{d}s + \left(\frac{\partial k}{\partial t}\right)\mathrm{d}t \tag{6}$$

Substituting this into Eq. 4 and using Eq. 6 results in the final equation for the motion of a curve representing the wavefront:

$$\frac{\partial k}{\partial t} + \left(\int_0^s Vk\,\mathrm{d}\xi + G\right)\frac{\partial k}{\partial s} = -Vk^2 - \frac{\partial^2 V}{\partial s^2} \tag{7}$$

where k is the curvature of the front parameterized by the arc length s.

The normal velocity $V_{(k)}$ is approximately a linear function in curvature. This was shown for a two-variable reaction-diffusion system (Zykov 1980) and also experimentally verified for a wide curvature range in a chemical reaction-diffusion system, the Belousov-Zhabotinsky reaction (Foerster et al. 1988). The linear equation takes the form

$$V(k) = V_0 - Dk \ , \tag{8}$$

where $V_0 = V_{(k=0)}$ and D is a positive parameter usually associated with a diffusion coefficient. The form of $G_{(k)}$ is in general not known. The theory of weakly excitable media can be found in a detailed review by Mikhailov et al. (1994) and the references therein.

4 Results

To describe the spatiotemporal development of an excitation wave by Eq. 7, one must specify V and G as functions of k. With the functions $V_{(k)}$ and $G_{(k)}$ the evolution of an arbitrary initial excitation pattern can then be calculated, at least numerically. An analytical solution is preferred but in general only possible for linear functions $V_{(k)}$ and $G_{(k)}$ and a symmetrical initial form of the wavefront.

It is not known in general how the tangential velocity G depends on the curvature k, but it is reasonable to expect that $G_{(k)}$ is monotonously decreasing with k just like $V_{(k)}$ (see Eq. 8). If we consider a limited curvature range Δk, we can assume a linear dependency for G on k in this range:

$$G = G_0\left(1 - \frac{k}{k_c}\right) \tag{9}$$

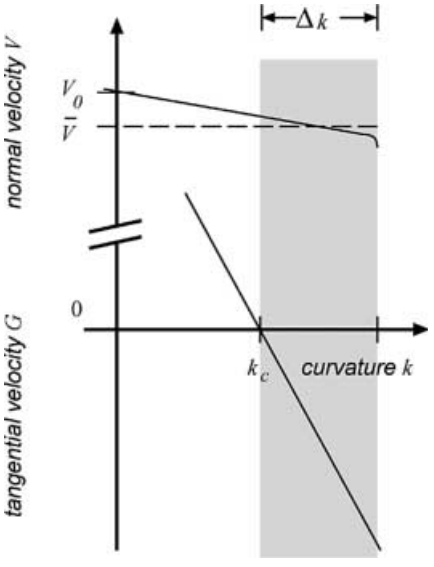

Fig. 3. Linearized functions of the normal velocity $V_{(k)}$ and of the tangential velocity of the free tip $G_{(k)}$ depending on curvature k. V_0 is the velocity of an uncurved wave front in the normal direction, and $\bar{V}$ is the average normal velocity in the curvature range Δk. The critical curvature k_c marks the lower bound of Δk beyond which free tips of a wave start to shrink. The analytical description of a weak excitable wave propagating in the cortex is valid within the *gray highlighted curvature* range Δk

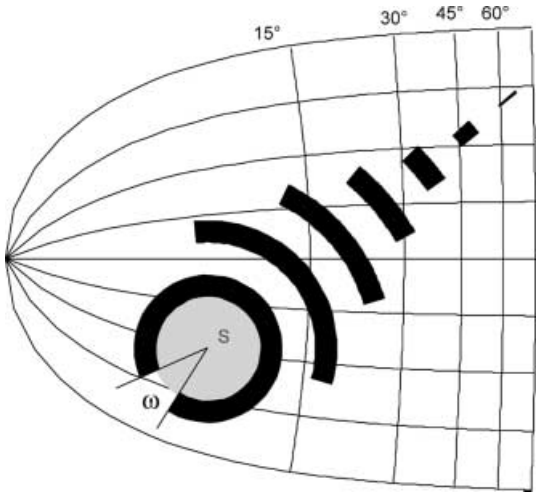

Fig. 4. The progression of a wave fragment within the primary visual cortex starting from an initial external stimulation S (*gray region*). The representation of the visual hemifield is shown by reverse logarithmic conformal mapping of a half disk. The focal point is offset by a spatial scale constant of 0.5

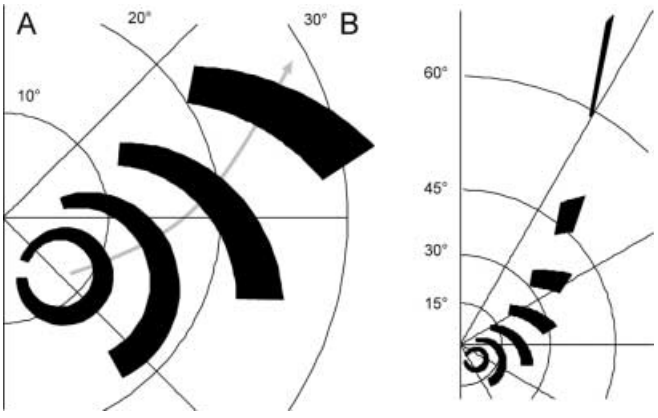

Fig. 5. a The progression of transient visual-field disturbances corresponding to the affected area in the primary visual cortex as shown in Fig. 4. The *black area* essentially marks the scotoma, whereas at the convex side a scintillating zig-zag pattern emerges (not shown). **b** The scotoma may take 20–25 min to expand from a sickle-shaped form near the center to the periphery of the visual hemifield, where the scotoma eventually disappears

with $G_0 = G_{(k=0)}$ and the parameter k_c as a critical curvature value. Before we look closer at this critical curvature, let us further assume that the function $V_{(k)}$ can be treated in the curvature range Δk as a constant $\bar{V}$ (Fig. 3). This is a reasonable assumption as long as the slope of the function $G_{(k)}$ is steeper than that of $V_{(k)}$ ($G_0/k_c \gg D$).

If the curvature at the free end of the wave equals the critical curvature ($k = k_c$), the tangential velocity G changes its sign and the growth rate of the end becomes negative, i.e., a contraction rate. This eventually leads to shrinkage of the length of the whole wave front, which can only be balanced by the stretching of a propagating convex wave front (Eq. 6).

After setting the functions $V_{(k)}$ and $G_{(k)}$ we still have to choose an initial excitation as the starting position of the wave before we can integrate Eq. 7. Since the medium is assumed to be homogeneous and isotropic, an initial excitation pattern must be introduced by an external stimulation S, as discussed later. We confine S to a single, circular region (Fig. 4) from whose edge a wave propagates outwards. Since the initial curvature of the front is highest, it may likely reach the value of the upper bound of Δk (Fig. 3). Beyond this curvature value wave propagation in the normal direction is not possible and the front becomes unstable. This can explain propagation failure at one or more positions, whereas in the following we choose, without loss of generality, a single place of propagation failure. At this position two open ends of the wave front occur, which overall results in a circle arc as the initial wave front location with an apex angle ω (Fig. 4).

Equation 7 can now be simplified and analytically integrated. Only the term leading to a change in arc length needs to be considered because the wave front will maintain the initially circular shape. Any indent caused by a fluctuation will be flattend because of the locally increased or decreased normal velocity for a wave fragment falling back or leading, respectively (Eq. 8). As described above, there are two counteracting effects acting on the total arc length. On the one hand, any increase in radius leads to a stretching of the curve and thus to an increase in arc length, and on the other hand, the negative growth rate at the open ends reduces the arc length. The second term on the left side of Eq. 7 considers both effects. Let us write this term in a slightly different but equivalent form. First, Eqs. 8 and 9 were inserted in Eq. 7. Second, the tangential velocity G is measured in units of $\bar{V}$, in other words, we set $\bar{V} = 1$. Finally, we introduce the radius r as the reciprocal of curvature k. Then we obtain

$$\frac{\mathrm{d}s}{\mathrm{d}r} = k_c \frac{s}{r} + G_0 \left(1 - \frac{1}{r}\right) \quad . \tag{10}$$

After integrating Eq. 10 and substituting the apex angle ω for the value s/r we get the formula

$$\omega = G_0 \left(\log(r) + \frac{1}{r} - 1\right) + \omega_c \quad . \tag{11}$$

The variable ω is used since its derivative with respect to r is directly proportional to the tangential velocity $G_{(k)}$. In Fig. 4 the wave is shown at seven subsequent locations, shrinking each time before it finally vanishes.

The evolution pattern of the weak excitation wave is fitted into the primary visual cortex and mapped onto a visual hemifield in the following way. Describing retinal and cortical coordinates with complex numbers, z and w, respectively, the retinocortical projection is given by the complex logarithmic function $w = \log(z + a)$ (Schwartz 1977). Usually an offset parameter $a > 0$ is introduced if the foveal region is considered. Since we are dealing with a hallucinatory vision, the map projection is used in reverse order, i.e., from cortex to retina (Ermentrout and Cowan 1979) and then map retinal coordinates to the visual field by perspective projection (Fig. 5).

The growth and form of the simulated scotoma up to an eccentricity of 30° matches those reported by migraine sufferers (Fig. 5). The form of a scotoma in the periphery of the visual field is hard to describe or even to draw for migraine sufferers and therefore has not yet been documented to our knowledge. Our model predicts that, while the scotoma is at the beginning sickle-shaped and roughly parallel to an azimuth, it eventually elongates in the radial direction before it finally disappears close to but not necessarily at the border of the visual field.

5 Discussion

The principle of pattern formation opens up to us a new view of the complexity of migraine aura symptoms. A pattern-formation process is, for example, the ability of the brain to form spatial representations of sensory information, which are commonly called cortical maps (Obermayer 2000). There is strong evidence that parts of an orientation map are literally seen by the migraineur as a zig-zag pattern when intense neurometabolic brain activity – as in the CSD condition – appears in cortex (Dahlem et al., 2000). The retinotopic map determines the growth of the visual migraine aura (Lashley 1941; Grusser 1995). However, the precise growth and form of the fortification figure is reflected not solely by reverse logarithmic mapping of apparent visual information. The underlying transient excitation pattern is governed by an independent pattern-formation process, which is the ability of the intense neurometabolic brain activity to propagate as a wave in a complex spatiotemporal fashion (Dahlem and Müller 1997).

One can model the zig-zag pattern of the fortification figure by a wave process, that is, without explicitly including cortical sensor maps (Reggia and Montgomery 1996). In this case the zig-zag pattern arises due to a front instability of the propagating wave. Apart from this, separate dynamics of the abnormal excitation in the cortex are in general ignored. To explain detailed features of the aura, e.g., the fading away of the symptoms in the periphery, cytoarchitectonic features are made responsible, e.g., the border between $V1$ and $V2$ was supposed to stop wave propagation (Grusser 1995). However, including cytoarchitectonic structures introduces inconsistencies. Why should a wave propagate in many different sensoric areas but not in $V2$?

We use two complementary pattern-formation processes to obtain a complete model of the fortification. On the one hand, there are the principles of cortical organization that govern the following aspects of the fortification: (1) the zig-zag pattern by the layout of orientation preference cells (Dahlem et al. 2000) and (2) the actual growth and form of the fortification figure in the visual field by complex logarithmic mapping. Statement 2 does not and cannot say anything about growth and form *before* the mapping from the visual cortex to the visual hemifield. For this we introduce, on the other hand, a process of active wave propagation in an excitable medium. Such a process governs many other features of the aura: (3) the excitation phase causes a positive neurological symptom (e.g., a zig-zag pattern), (4) the refractory phase causes a negative symptom (e.g., a scotoma), (5) negative symptoms must always appear after positive symptoms in sensory space, and (6) negative symptoms are usually much longer lasting and cover a larger sensory region at a time; finally, (7) curvature effects explain confined appearance of the symptoms in sensory space.

Within the framework of weakly excitable media is an alternative explanation to the curvature-induced propagation failure. Just like wave-front curvature, the convoluted surface of the cortex affects wave velocity. One must differentiate between positive and negative Gaussian curvature of the cortex surface. A surface that bulges out in all directions, such as the surface of a sphere, is positively curved; a saddle-shaped surface has negative Gaussian curvature. A wave that propagates into a region of increasing Gaussian curvature accelerates as if the wave front were positively curved (Davydov and Zykov 1991). If the wave propagates into decreasing Gaussian curvature, its velocity decreases. The latter effect can contribute to the propagation failure of the wave. Thus an extended model for wave propagation on curved surfaces can explain – in a way similar to how we have shown here for curved wave fronts – why CSD waves are limited in spread by the complexly gyrate nature of human brain (James et al. 1999) and why they may not cross prominent sulci (Hadjikhani et al. 2000).

There remain at least two unanswered questions: How is a single sensory aura stimulated in the first place? And why is there sometimes a sequence of disturbances, e.g., from visual to tactile to language? No direct answers to these questions can be formed from our model equation since those questions concern its initial condition. However, there is in the framework of excitable media a consistent picture. Recent studies have generally led to the conclusion that migraine with aura is associated with a state of functional cortical hyperexcitability (Aurora and Welch 1998; Palmer et al. 2000). Although *functional* cortical excitability is not defined in the same way as excitability in the theory of excitable media, it is reasonable to assume that they correlate. In the case of increased functional excitability, the excitability approaches the boundary of wave propagation ∂P. A further shift of excitability into the regime of wave propagation would then cause a migraine aura attack that would develop in the way we have shown here. This shift may be caused by the well-known migraine triggers, but interestingly the visual aura is also evoked by scintillating visual stimuli (Hadjikhani et al. 2000).

Why is there sometimes a sequence of disturbances, e.g., from visual to tactile to language? Cortical areas have a different susceptibility to CSD waves – and therefore to sensory aura, too. If an attack is triggerd globally via blood vessels, as generally assumed, the aura should then occur in the order of decreasing susceptibility. Some sensory areas may not be involved at all, depending on the strength of the attack.

It was long challenged that CSD underlies migraine aura, but recent studies have further established CSD

as a migraine model (Bolay et al. 2002), and the clinical relevance of CSD can no longer be doubted (Gorji 2001). Our mathematical model also provides strong support for an excitable wave hypothesis of migraine aura and reveals the relation between cortical sensor maps and traveling waves in migraine. A fruitful endeavor will be an investigation of functional cortical excitability compared to excitability as introduced here.

Acknowledgements. We would like to thank V. Zykov for useful discussions on wave Propagation, and one of us (MAD) would like to thank Ed Chronicle for useful discussions on functional excitability. This project was supported by a scholarship Landesstipendium Sachsen-Anhalt to MAD.

References

Aurora SK, Welch KM (1998) Brain excitability in migraine: evidence from transcranial magnetic stimulation studies. Curr Opin Neurol 11: 205–209

Aurora SK, Welch KM (2000) Migraine: imaging the aura. Curr Opin Neurol 13: 273–276

Bolay H, Reuter U, Dunn AK, Huang Z, Boas DA, Moskowitz MA (2002) Intrinsic brain activity triggers trigeminal meningeal afferents in a migraine model. Nat Med 8: 136–142

Brazhnik PK, Davydov VA, Mikhailov AS (1988) Kinematical approach to description of autowave processes. Theor Math Phys 74: 300–306

Bureš J, Burešova O, Křivánek J (1974) The mechanism and application of Leao's spreading depression of electroencephalographic activity. Academic, New York

Dahlem MA, Müller SC (1997) Self-induced splitting of spiral-shaped spreading depression waves in chicken retina. Exp Brain Res 115: 319–324

Dahlem MA, Engelmann R, Löwel S, Müller SC (2000) Does the migraine aura reflect cortical organization? Eur J Neurosci 12: 767–770

Davydov VA, Zykov VS (1991) Kinematics of spiral waves on nonuniformly curved surfaces. Physica D 49: 71–74

Ermentrout GB, Cowan JD (1979) A mathematical theory of visual hallucination patterns. Biol Cybern 43: 137–150

Foerster P, Müller SC, Hess B (1988) Curvature and propagation velocity of chemical waves. Science 241: 685–687

Gorji A (2001) Spreading depression: a review of the clinical relevance. Brain Res 38: 33–60

Grusser OJ (1995) Migraine phosphenes and the retino-cortical magnification factor. Vision Res 35: 1125–1134

Hadjikhani N, Sanchez Del Rio M, Wu O, Schwartz D, Bakker D, Fischl B, Kwong KK, Cutrer FM, Rosen BR, Tootell RB, Sorensen AG, Moskowitz MA (2000) Mechanisms of migraine aura revealed by functional MRI in human visual cortex. Proc Natl Acad Sci USA 98: 4687–4692

James MF, Smith MI, Bockhorst KH, Hall LD, Houston GC, Papadakis NG, Smith JM, Williams AJ, Xing D, Parsons AA, Huang CL, Carpenter TA (1999) Cortical spreading depression in the gyrencephalic feline brain studied by magnetic resonance imaging. J Physiol 519: 415–425

Kapral R, Showalter K (eds) (1995) Chemical waves and patterns. Kluwer, Dordrecht

Lashley K (1941) Patterns of cerebral integration indicated by scotomas of migraine. Arch Neurol Psychiatry 46: 331–339

Launer LJ, Terwindt GM, Ferrari MD (1999) The prevalence and characteristics of migraine in a population-based cohort: the GEM study. Neurology 53: 537–542

Lauritzen M (1994) Pathophysiology of the migraine aura: the spreading depression theory. Brain 117: 199–210

Leão AAP (1944) Spreading depression of activity in the cerebral cortex. J Neurophysiol 7: 359–390

Mikhailov AS, Davydov VA, Zykov VS (1994) Complex dynamics of spiral waves and motion of curves. Physica D 70: 1–39

Nagy-Ungvarai Zs, Ungvarai J, Müller SC (1994) Complexity in spiral wave Dynamics. Chaos 3: 15–19

Obermayer K (2000) Modeling the formation of sensory representations in the brain. In: Cruse H, Dean J, Ritter H (eds) Prerational intelligence: adaptive behavior and intelligent systems without symbols and logic, vol 1. Kluwer, Dordrecht, pp 215–232

Palmer JE, Chronicle EP, Rolan P, Mulleners WM (2000) Cortical hyperexcitability is cortical under-inhibition: evidence from a novel functional test of migraine patients. Cephalalgia 20: 525–532

Reggia JA, Montgomery D (1996) A computational model of visual hallucinations in migraine. Comput Biol Med 26: 133–141

Richards W (1971) The fortification illusions of migraines. Sci Am 224: 88–96

Russell MB, Olesen J (1996) A nosographic analysis of the migraine aura in a general population. Brain 119: 355–361

Schwartz E (1977) Spatial mapping in the primate sensory projection: analytic structure and relevance to perception. Biol Cybern 25: 181–194

Wiener N, Rosenbluth A (1946) The mathematical formulation of the problem of conduction of impulses in a network of connected excitable elements, specifically in cardiac muscle. Arch Inst Cardiol Mexico 16: 205–265

Wilkinson M, Robinson D (1985) Migraine art. Cephalalgia 5: 151–157

Winfree AT (1991) Varieties of spiral wave behaviour: an experimentalist's approach to the theory of excitable media. Chaos 1: 303–334

Zykov VS (1980) Analytical estimate of the dependence of the excitation wave velocity of the curvature of its front in a two dimensional medium. Biophysics (USSR) 25: 906–912